Macromolecules

Cite This: Macromolecules XXXX, XXX, XXX−XXX

Article

pubs.acs.org/Macromolecules

Dynamic Cross-Linking of Polyethylene via Sextuple Hydrogen Bonding Array

Jonathan Tellers,[†] Stefano Canossa,[†] Roberta Pinalli,[†] Maria Soliman,[‡] Jérôme Vachon,*[,‡] and Enrico Dalcanale*[,†]

[†]Department of Chemistry, Life Sciences and Environmental Sustainability and INSTM UdR Parma, University of Parma, Parco Area delle Scienze 17/A, 43124 Parma, Italy

[‡]SABIC Europe B.V., Urmonderbaan 22, 6160 AH Geleen, The Netherlands

Supporting Information

ABSTRACT: Multiple hydrogen bonding motifs are promising tools for polymer functionalization to obtain adaptable networks combining advantages of permanently cross-linked systems with processability of thermoplastics. Here we describe the use of a new multiple hydrogen bonding motif to impart increased tensile strength, stiffness, barrier properties, and a plateau modulus after melting to functional polyolefins, while retaining adaptability of the polymer network. The cross-linked nature of these polymers was elucidated by thermal and mechanical analysis, revealing a raised glass transition and rheology similar to permanently cross-linked polymer matrices. The apolar polymer matrix was found to stabilize the new hydrogen bonding motif at elevated temperatures. The resulting polymer showed thermal resistance superior to ureidopyrimidone (UPy) motif functionalized materials, the most commonly employed synthetic multiple hydrogen bonding motif to date.

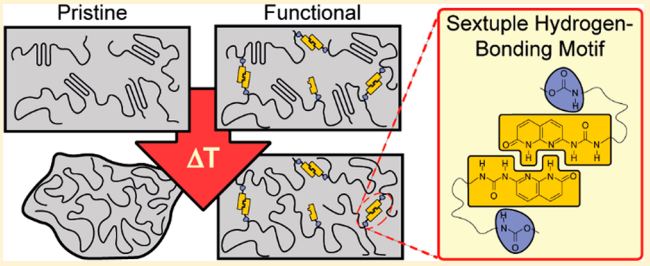

INTRODUCTION

Polyethylene (PE) is the most widely employed synthetic polymer in the world,[1,2] owing to its low cost and excellent properties such as chemical resistance, processability, moisture resistance, and low conductivity.[3] However, there is an ongoing interest to overcome some of the flaws of PE such as wear,[4,5] poor oxygen barrier properties,[6,7] low strength,[8,9] and creep,[8,10] relying mostly on fillers as property enhancing tool.

The introduction of hydrogen bonding in polymers can lead to extraordinary properties. For example, nylon, possibly described as a PE backbone chain with equally spaced difunctional hydrogen bonding moieties (amides), has superior tensile, barrier, fatigue, and heat resistance properties.[11−13] Ethylene vinyl alcohol (EVOH) shows superior barrier properties ascribed to a high crystallinity resulting from the considerable cohesive energy between chains provided by the large amount of hydrogen bonds present.[14] Other notable examples of polymers that own some of their remarkable properties to hydrogen bonding are polyurea and polyurethanes.[15] The properties of these polymers are however profoundly dependent on moisture, as it can interfere with the hydrogen bonds.[16−19]

More recently, arrays of multiply hydrogen bonds have been explored to improve polymer properties. These are molecules inspired by DNA base pairs with a favorable arrangement of hydrogen bonding donor (D) and acceptor (A) groups, allowing for organized self-assembly.[20] Following this concept, molecules with a plethora of different structures were developed with the ability to homo- or heterodimerize.[20−22] Using multiple hydrogen bonding moieties, properties such as controlled degradation,[23] optical responsiveness,[24] high strength and stiffness,[25] increased peel strength,[26] self-healing,[27] miscibility between immiscible polymers,[28] and reversible chain extension[29,30] can be introduced into polymers. The increased strength of these hydrogen bonding arrays can lead to their assembly even in water,[31,32] thus making them an excellent tool for the preparation of humidity and moisture resistant materials.

Among the different types of multiple hydrogen bonding array molecules, the most prominent is the ureidopyrimidone (UPy)[29] motif, a self-dimerizing quadruple hydrogen bonding motif characterized by a high association constant,[33] ease of synthesis,[34] and readily available derivatives for functionalization of polymers.[35] To date, UPy has been the most important studied synthetic multiple hydrogen bonding motif.[36] Research on polymers functionalized with UPy has largely been focused on telomers at lab scale, while functionalization of long chain polyolefins remains largely unexplored. Coates et al. polymerized 1-hexene with alkene functionalized UPy, obtaining a completely amorphous, wax-like polyolefin with improved tensile properties over nonfunctionalized homopolymer.[37]

Received: August 8, 2018
Revised: September 7, 2018

DOI: 10.1021/acs.macromol.8b01715
Macromolecules XXXX, XXX, XXX−XXX

Nojiri et al. reported a UPy functionalized polypropylene (PP),[38] where melt viscosity was increased after functionalization with UPy units. The reported dissociation temperature of UPy moieties is at 190 °C, which is about 40 °C higher than the degradation temperature of UPy moieties reported in the literature.[35,39] Additionally, they described the compatibilization of isotactic polypropylene functionalized with UPy and ethylene-*co*-propylene functionalized with Napy, using the ability of these moieties to form heterodimers.[40] Here, melt mixing of polymers was performed at 170 and 210 °C, exceeding the reported temperature of degradation of UPy in polymers by 20 and 60 °C, respectively. Together, this raises concerns about the chemical integrity of the analyzed polymer samples.

The development of alternative, more temperature stable H-bonding motifs is desirable. Herein, we report the development of the novel self-dimerizing multiple hydrogen bonding array 1-(7-oxo-7,8-dihydro-1,8-naphthyridin-2-yl)urea (ODIN, Figure 1, compounds **3** and **4**) with a DDADA binding motif able

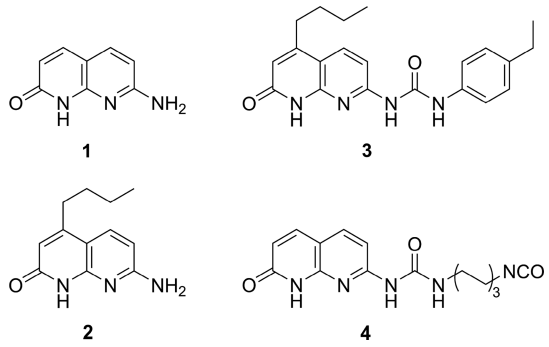

Figure 1. Overview of employed naphthyridine derivatives.

to form dimers in the solid state. Introduction of ODIN into poly(ethylene-*co*-(2-hydroxyethyl methacrylate)) (PE-HEMA), a functional polyethylene with pendant hydroxy groups, gives rise to improved mechanical and barrier properties, an increased melt strength, and improved thermal stability compared to UPy functionalized polymers.

METHODS

General. *Nuclear Magnetic Resonance (NMR).* NMR spectra were recorded on a Bruker AVANCE 400 (400 MHz) spectrometer and a Bruker AVANCE 300 (300 MHz) at room temperature. Chemical shifts are reported in parts per million (ppm). ^{1}H NMR chemical shifts are given in reference to the residual solvent peak at 7.26 ppm in $CDCl_3$ and at 2.50 ppm in DMSO-d_6. High-temperature NMR spectra were recorded on a Bruker AVANCE III (500 MHz) equipped with a cryogenically cooled probe head at 120 °C in deuterated tetrachloroethane (TCE-d_2). ^{1}H NMR chemical shifts are given in reference to the residual solvent peak of TCE at 6.00 ppm.

Infrared Spectroscopy (IR). IR spectra were recorded on a PerkinElmer Spectrum One equipped with a Golden Gate accessory (diamond ATR). Variable temperature IR (VTIR) spectra were recorded on a Bruker Vertex 70 spectrometer equipped with a diamond ATR accessory (GladiATR 300 by PIKE Technologies). First, spectra were recorded of the empty crystal at all employed temperatures. These spectra were subsequently used as background spectra for the actual measurements to compensate for the change in transmission of diamond at elevated temperatures.

Elemental Analysis (EA). A small amount of sample is burned in the presence of oxygen. The nitrogen content was determined by means of thermal conductivity (TC) and volumetric analysis. The hydrogen and carbon contents were determined by NIR.

Single Crystal X-ray Diffraction (SCXRD). SCXRD analysis was performed at the ELETTRA Synchrotron facility (XRD1 beamline).[41] Diffraction data were collected using a monochromatic 0.7 Å wavelength at 100 K, using an Oxford Cryostream 700[42] cooling device. Diffraction data sets were processed using CrysAlisPro software ver. 1.171.38.43.[43] Structure solution and refinement were conducted using Olex2 software ver. 1.2.9.[44] CCDC 1825490 contains crystallographic data relative to the described phases. This data can be obtained free of charge from the Cambridge Crystallographic Data Centre via https://www.ccdc.cam.ac.uk/structures.

Gel Permeation Chromatography (GPC). GPC was performed on a Polymer Char GPC-IR system using a Polymer Char IR 5 infrared detector as concentration detector and a Wyatt MALLS detector Helios II. As column set two Polymer laboratories 20 μm PLgel MIXED ALS (300 × 7.5 mm) were used. System performance is safeguarded by measuring the statistical process control sample (SPC) NBS 1475A (or PE52K) and STAM 7625 before every sample series. Samples were dissolved in *o*-dichlorobenzene, and the runs were performed at 160 °C.

Differential Scanning Calorimetry (DSC). DSC was performed on a TA Instruments Q20 equipped with a RCS 90 cooling system. About 3−5 mg of polymeric sample was weighed inside an aluminum pan and subjected to DSC measurements under a nitrogen atmosphere. Unless otherwise noted, polymers were screened twice from −90 to 200 °C at a constant heating/cooling rate of 10 K/min. Melting and glass transition (T_g) temperatures and the enthalpy of melting were determined from the second heating, crystallization temperature from the second cooling cycle.

Tensile Tests. Tensile tests were performed on a Zwick type Z100 tensile tester equipped with a 100 N load cell. Specimens were obtained by cutting strips of 8 cm length and 1 cm width from square films (10 × 10 cm^2) with an average thickness of 150 μm. Sample strips were clamped, and a preload of 0.3 MPa was applied before stretching at a speed of 200 mm/min until sample failure occurred.

Compression Molding. Polymer films and samples for DMTA and rheology were obtained by following the subsequent protocol: Appropriate molds were filled with the polymer powder, followed by treating the material in a preheating step for 5 min at 150 °C, then for 10 min at 150 °C with an applied force of 50 kN, and finally cooling at a rate of 15 K/min until a temperature of 40 °C was reached while maintaining the applied force.

DMTA Measurements. Rectangular samples suitable for DMTA were cut to dimensions of 3 × 5 × 0.5 mm^2 (length × width × thickness). Samples were measured on a TA Instruments Q800 in tensile mode. The storage modulus (E') and loss modulus (E'') were monitored while screening the samples during a temperature sweep from −100 to 200 °C at 3 K/min. An oscillation frequency of 1 Hz with an oscillation amplitude of 10 μm was applied.

Rheology. Samples for rheology were prepared via compression molding to obtain disk shaped specimens (diameter 25 mm, thickness 1 mm). Samples were measured using a TA Instruments DHR-2, equipped with a parallel plate geometry. Samples were measured with a frequency sweep from 100 to 0.01 rad/s using a strain amplitude of 0.4% at a temperature of 150 °C.

Oxygen and Water Transmission. At least two films were measured for each sample, and obtained transmissions are reported as the average of both measurements. Oxygen transmission rates were determined according to ISO 15105-2 at 23 °C, 0% relative humidity (rh) and at 38 °C, 50% rh. Water vapor transmission rates were determined at 23 °C and 85% rh, adhering to the ISO 15106-3 standard. The thickness of films, ranging from 100 to 120 μm, was measured at varying locations, and the average was used to report thickness corrected oxygen transmission rates.

Synthesis. Unless otherwise specified, chemicals and solvents were purchased from Sigma-Aldrich and used as received. The poly(ethylene-*co*-(2-hydroxethyl methacrylate)) copolymers were provided by SABIC. All solvents employed were laboratory grade and used as received. An overview of the prepared naphthyridine derivatives is displayed in Figure 1.

DOI: 10.1021/acs.macromol.8b01715
Macromolecules XXXX, XXX, XXX−XXX

*7-Amino-1,8-naphthyridin-2(1H)-one (**1**).* Naphthyridine **1** was synthesized according to the literature.[45] Ground diaminopyridine (109.13 g, 0.98 mol, 1 equiv) and malic acid (145 g, 1.08 mol, 1.1 equiv) were placed in a three-neck flask and cooled in an ice bath. Sulfuric acid (500 mL) was slowly added while maintaining an internal temperature below 45 °C. The obtained mixture was slowly heated to 110 °C and reacted for 2.5 h. Subsequently, after cooling the mixture, the lukewarm solution was poured over ice, and concentrated ammonia (~1.5 L) was slowly added while stirring until a pH of ~7−8 was reached. The precipitate was filtered and first washed with ~9 L of water and then with a mixture of H_2O and MeOH (9:1) until the wash was colorless. The solid residue was dried under vacuum at 100 °C to obtain the product as a deep brown solid (133.2 g, 84% yield). The characterization gave values consistent with the literature.[45] ^{1}H NMR (300 MHz, DMSO-d_6) δ: 11.85 (s, 1H), 7.65 (d, J = 9.3 Hz, 2H), 7.64 (d, J = 8.6 Hz, 1H), 6.34 (d, J = 8.5 Hz, 1H), 6.11 (d, J = 9.2 Hz, 1H).

*7-Amino-4-butyl-1,8-naphthyridin-2(1H)-one (**2**).* The synthesis for **2** was adapted from the literature.[46] A three-neck flask equipped with a thermometer, mechanical stirrer, and dropping funnel was charged with diaminopyridine (12.67 g, 1 equiv) and methyl 3-oxoheptanoate (20.20 g, 1.1 equiv) and stirred for 1 h. The mixture was then cooled to 0 °C, and sulfuric acid (65 mL) was slowly added while maintaining a temperature below 45 °C. After full addition the dropping funnel was replaced with a reflux condenser, and the mixture was heated for 1.5 h at 120 °C. The solution was then cooled to room temperature, poured over ~100 g of ice, and brought to pH ~ 7−8 by slow addition of a 30% ammonia solution (~125 mL). The formed precipitate was filtered, washed with water, then triturated with a 1:9 methanol/water mixture, filtered again, and washed with methanol/acetone until the wash was colorless. The product was dried under vacuum and obtained as a yellow solid (10 g, 40% yield), which was used immediately without further purification. MS (ESI) m/z: $[M + H]^+$ calcd for $C_{12}H_{15}N_3O$, 218.13; found, 218.09.

*1-(5-Butyl-7-oxo-7,8-dihydro-1,8-naphthyridin-2-yl)-3-(4-ethylphenyl)urea (**3**).* **2** (0.1 g, 0.46 mmol, 1 equiv) and 4-ethylphenyl isocyanate (0.3 mL, 2.1 mmol, 4.6 equiv) were combined in a 10 mL vial and stirred overnight at 110 °C. A 1:1 hexane/acetone mixture (5 mL) was added, and the precipitate was filtered off and washed with acetone until the wash was colorless. The compound was dried under vacuum and obtained as a tan powder (0.106 g, 63% yield). Crystals shaped like needles suitable for X-ray crystallography were obtained from **3** dissolved in chloroform and layered with acetone. ^{1}H NMR (300 MHz, DMSO-d_6) δ: 12.26 (s, 1H), 10.56 (s, 1H), 9.87 (s, 1H), 8.11 (d, J = 8.7 Hz, 1H), 7.62 (d, J = 8.5 Hz, 2H), 7.16 (d, J = 8.4 Hz, 2H), 7.07 (d, J = 8.7 Hz, 1H), 6.24 (s, 1H), 2.74 (t, J = 7.6 Hz, 2H), 2.58 (q, J = 7.6 Hz, 2H), 1.64−1.51 (m, 2H), 1.38 (m, 2H), 1.18 (t, J = 7.6 Hz, 3H), 0.92 (t, J = 7.3 Hz, 3H). MS (ESI) m/z: $[M + H]^+$ calcd for $C_{21}H_{24}N_4O_2$, 365.20; found, 365.23.

*1-(6-Isocyanatohexyl)-3-(7-oxo-7,8-dihydro-1,8-naphthyridin-2-yl)urea (**4**).* Naphthyridine **1** (50 g, 0.31 mol, 1 equiv) and hexamethylene diisocyanate (500 mL, 3.1 mol, 10 equiv) were combined and stirred. The resulting slurry was heated for 15 h at a temperature of 118 °C (temperature of oil bath). After cooling to room temperature, the solid was filtered over a Buchner funnel and washed with hexane and acetone until the wash was colorless. The solid residue was dried under vacuum at 60 °C, yielding the product as a tan powder with minor impurities (72.7 g, 71% yield). ^{1}H NMR (400 MHz, DMSO-d_6) δ: 12.18 (s, 1H, Ar−N*H*), 9.65 (s, 1H, Ar−N*H*−CO−NH), 8.99 (s, 1H, N*H*−CO−NH−Ar), 7.91 (d, J = 8.4 Hz, 1H), 7.78 (d, J = 9.4 Hz, 1H), 6.84 (d, J = 8.5 Hz, 1H), 6.34 (d, J = 9.4, 1.8 Hz, 1H), 3.39−3.31 (m, 2H), 3.20 (dd, J = 6.7 Hz, 2H), 1.62−1.48 (m, 4H), 1.43−1.19 (m, 4H). MS (ESI) m/z: $[M + H]^+$ calcd for $C_{17}H_{23}N_5O_4$ (methanol adduct), 362.18; found, 362.26.

*Synthesis of Polymers **P1**−**P4**.* PE−HEMA copolymers were functionalized according to the following general procedure: PE−HEMA (4 g) was dissolved under a nitrogen atmosphere in toluene (200 mL) at 80 °C for 1 h inside a custom-made glass reactor equipped with mechanical stirring, cooling, and gas inlet. The apparatus was flushed with nitrogen, and **4** (1.3 equiv with respect to hydroxy groups) was added as a solid, followed by addition of 4 drops of dibutyltin dilaurate (DBTDL) as catalyst. The temperature of the mixture was raised to 100 °C and stirred for 4 h. The hot suspension was filtered through a preheated (140 °C) Buchner funnel to filter off residual unreacted **4** and immediately precipitated into isopropanol. The precipitate was dried under vacuum to obtain polymers **P1**−**P4** as off-white to yellow solids.

RESULTS AND DISCUSSION

Design and Preparation of 1-(7-Oxo-7,8-dihydro-1,8-naphthyridin-2-yl)urea (ODIN), a Novel Multiple Hydrogen Bonding Motif. As the most ubiquitous self-dimerizing multiple hydrogen bonding motif to date,[47,48] we first considered the quadruple hydrogen bonding motif ureidopyrimidinone (UPy)[49] (Figure 2A) for the preparation of

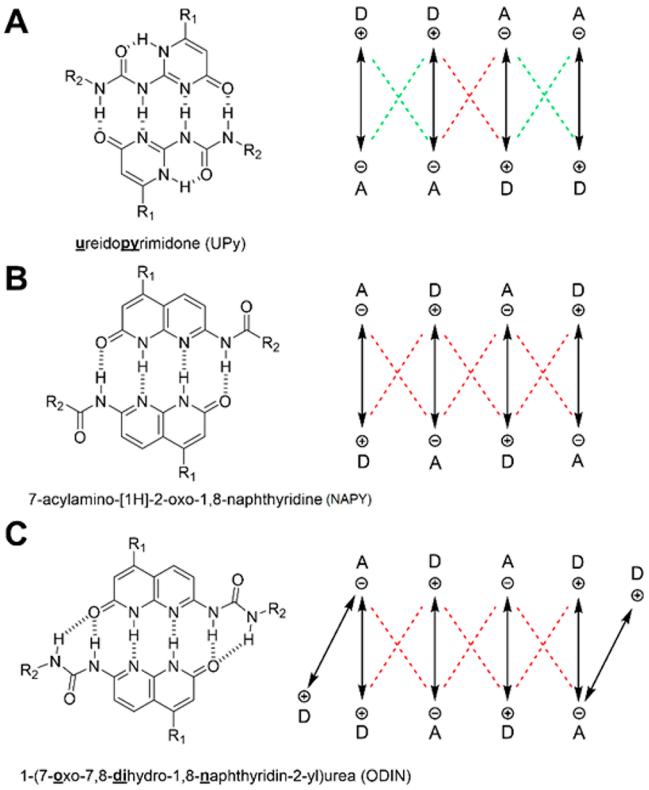

Figure 2. Structures of (A) ureidopyrimidinone (UPy) motif,[49] (B) 7-acylamino-[1*H*]-2-oxo-1,8-naphthyridine (NAPY),[54] and (C) the naphtyridine based motif ODIN. On the right, the respective arrangements of donor (D) and acceptor (A) moieties as well as attractive (green dotted) and repulsive (red dotted) secondary electrostatic interactions (according to Jorgensen[55,56]) are illustrated.

functional polyolefins. However, because of concerns about thermal stability due to the UPy urea bond being cleaved at elevated temperatures[50,51] and a degradation temperature of UPy moieties in polymers given at ~150 °C,[35] we desired an alternative. Some of the UPy degradation compounds have been identified as isocyanate species,[50,52] which form as a result of the thermoreversible nature of the urea moiety.[53]

It has been shown that urea thermal stability and extent of electron delocalization in aryl-substituted urea can be correlated.[57] Thereby, extending the conjugation of the aryl substituent (in the case of UPy the substituent can be viewed as isocytosine) might result in a more temperature stable urea. One way to extend the conjugated system is by employing

DOI: 10.1021/acs.macromol.8b01715
Macromolecules XXXX, XXX, XXX−XXX

fused aromatic species.[58] Naphthyridines, a class of heterocycles made up of two fused aromatic rings,[59] could provide a suitable alternative to UPy. For example, a known quadruple hydrogen bonding motif can be obtained by acylation of naphthyridine **1** (Figure 2B).[54,60] NAPY dimerizes via an alternating DADA arrangement of donors and acceptors with an association constant (K_a) of ~750−1900 M^{-1} (in $CHCl_3$), dependent on the side chain.[54] The comparatively weak association constant was desired because already 1−2 mol % of weakly hydrogen bonded dimers is sufficient to affect the mechanical behavior in thermoplastics substantially.[61,62] An array of at least four hydrogen bonds should be maintained to ensure association in the presence of water.[31,32] To facilitate the introduction of these hydrogen bonding arrays into functional polymers with little synthetic effort, an excess of diisocyanate was employed to react with the free amine group of **1**, forming **4** with an urea link and free aliphatic isocyanate available for functionalization. The introduction of the urea group provides an additional hydrogen bonding donor that can interact with one of the oxygen lone pairs of the lactam, resulting in a self-assembly mode involving six hydrogen bonds (Figure 2C, the ODIN motif). The assembly mode of ODIN was elucidated by synthesizing derivative **3** with an increased solubility in organic solvents, needed to grow single crystals. Compound **3** presents the same DDADA arrangement of donor and acceptor groups as **4**, specifically an urea group with two N−H as donor, an aromatic N as acceptor, and a lactam N−H donor, C═O acceptor moiety. The K_a of ODIN was investigated by fluorescence measurements of **3** dissolved in $CHCl_3$ (see Supporting Information for method and Figure S1), from which a K_a of 4×10^4 M^{-1} (in $CHCl_3$) was determined for ODIN dimerization. The crystal structure of **3** reveals the formation of dimers that stack head to tail driven by the self-complementary DDADA arrangement (Figure 3A). As consequence the molecules are coplanar, and their mutual disposition allows for the formation of two bifurcated hydrogen bonds between both urea N−H donor moieties and the oxygen of the lactam, while the aromatic nitrogens are involved with the aromatic N−H groups of the respective molecular counterparts of the dimer. The only heteroatoms not involved in the intradimer interactions are the oxygen atoms of the urea group, which accept weak hydrogen bonds from the aliphatic C−H groups belonging to adjacent dimers (Figure 3B).

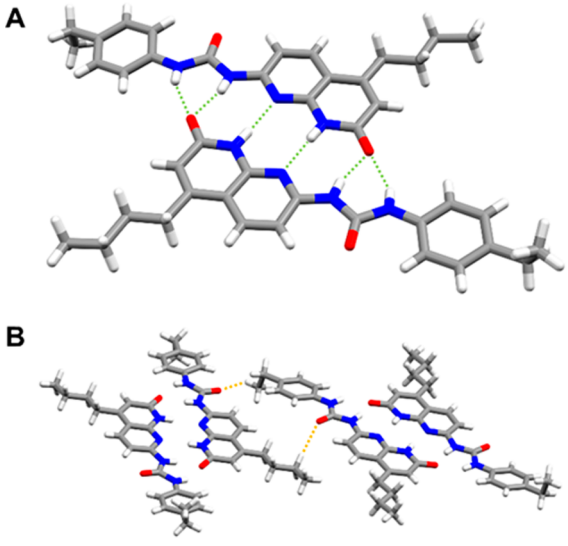

Figure 3. Dimeric structure of **3** (A) and its interactions with adjacent dimers (B), as observed in the crystalline phase. The intradimer and interdimer hydrogen bonds are highlighted in light green and orange, respectively.

The intermolecular interaction energy of the dimer of **3** observed in the solid state was calculated using the program Crystal Explorer.[63] According to the adopted methods (see Supporting Information), the total energy of the dimeric unit amounts to −166.8 kJ/mol. Analogous calculations were performed considering the two different dimeric forms discussed previously (A and B in Figure 2), showing −116.3 kJ/mol for the DADA and −203.5 kJ/mol for the DDAA type. As a matter of fact, the most stabilizing interaction can only be achieved avoiding alternation of donor and acceptor groups. Indeed, although for the dimer of **3** the greater number of interactions could potentially lead to a better stabilization, both studies in the solid state and in solution reveal that the DDADA sequence results into a less effective association than the DDAA (UPy $K_a = 2 \times 10^7$ M^{-1} in $CHCl_3$).[33] This aspect has already been addressed by Jorgensen et al. on the basis of *ab initio* computational studies,[55] experimentally confirmed by Zimmerman et al.,[56] and the present evidence further confirms the applicability of this rule to the cited systems.

Synthesis of Multiple Hydrogen-Bonding Functionalized PE Polymers. For the preparation of a multiple hydrogen bonding cross-linked polyolefin, polymers bearing moieties suitable for grafting of the hydrogen bonding motifs are required. Because ODIN motif **4** (Figure 1) bears an aliphatic isocyanate, polymers with pendant hydroxy or amino groups were considered. PE−HEMA, a copolymer of ethylene and 2-hydroxyethyl methacrylate (structure in Figure 4A), is available from SABIC with HEMA content ranging from 1.6 to 12.4 mol %. The pendant hydroxy groups of HEMA allow for easy grafting of the isocyanate **4**.[64−66] A homopolymeric PE sample, prepared employing the same reaction conditions that were used to synthesize PE−HEMA, was used as a reference material. The provided copolymers used in this study, their HEMA content in mol % determined via NMR, their molecular weight determined by GPC (traces reported in Figure S2), T_m determined via DSC (graphs in Figure S3), and T_β obtained from DMTA are reported in Table 1.

The synthesis pathway for the formation of multiple hydrogen bonded semicrystalline LDPE is depicted in Figure 4A. The reaction was carried out for 4 h at 100 °C in toluene with DBTDL acting as a catalyst. An overview of the prepared functional polymers **P1**−**P4**, the content of introduced ODIN determined via either NMR or elemental analysis (EA), and some characteristic thermal data are given in Table 2.

Molecular weight was not determined after functionalization due to solubility issues in *o*-dichlorobenzene. Because of the nature of cross-linking via multiple hydrogen bonding moieties, the virtual molecular weight should increase, reflected by the decreased solubility.[68] ^{1}H NMR of **P1**−**P4** in TCE-d_2 at 120 °C revealed the characteristic, strongly downfield shifted signals corresponding to amine protons participating in multiple hydrogen bonding (Figure 4B).[69] The degree of functionalization could be investigated via ^{1}H NMR by following the intensity of the HEMA methylene signals ($\delta \sim$ 3.85 and 4.25 ppm). A selected portion of the ^{1}H NMR spectrum for **P1**, detailing the hydroxyethylene methylene signals, is shown in Figure 4C. The two distinct methylene

DOI: 10.1021/acs.macromol.8b01715
Macromolecules XXXX, XXX, XXX−XXX

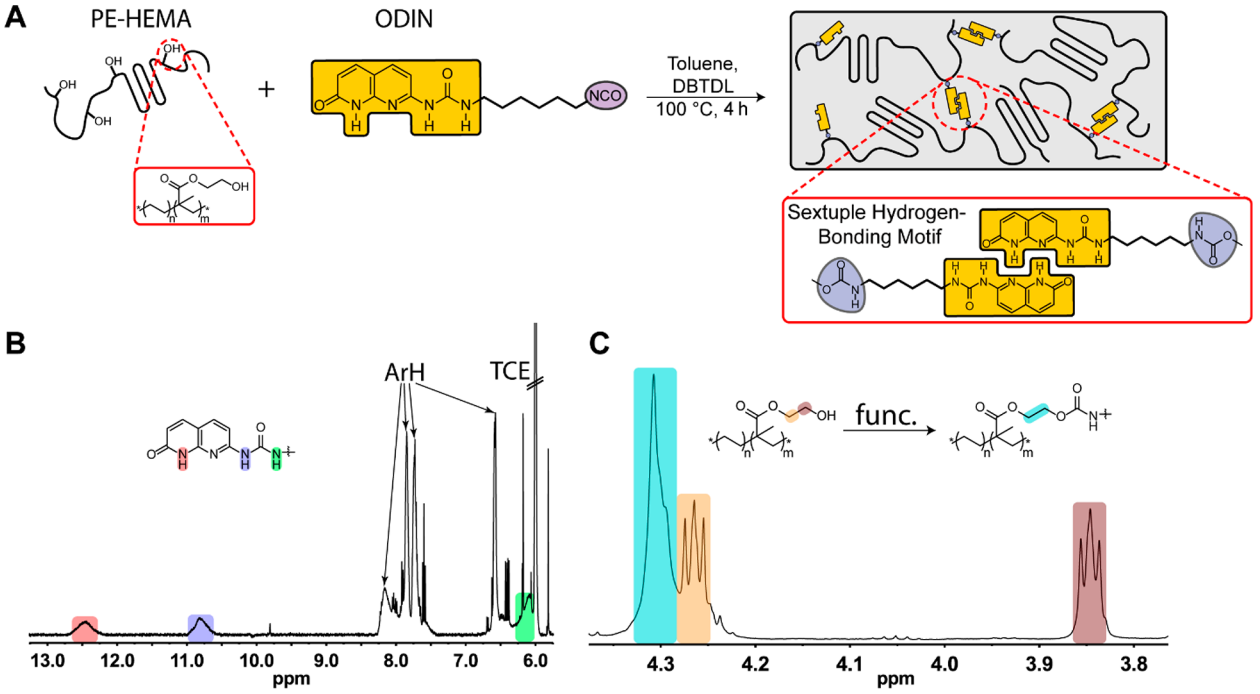

Figure 4. (A) Synthesis of hydrogen bonding functionalized PE−HEMA; cartoon depicts semicrystalline nature of resulting polymer cross-linked via multiple hydrogen bonding moieties. (B) Selected portion of P1 ^{1}H NMR (120 °C, in TCE-d_2) highlighting the hydrogen bonding region; signal of CH−N*H* is superimposed by the residual solvent TCE signal. (C) Selected portion of P1 ^{1}H NMR (120 °C, TCE-d_2), highlighting the HEMA hydroxyethyl signal region; the methylene groups of functionalized HEMA give rise to only a single signal.

Table 1. HEMA Content, GPC Data, and Thermal Data for PE−HEMA Copolymers

entry	HEMA[a] (mol %)	M_w[b,c] (kg/mol)	PDI[b]	T_m[d] (°C)	T_β[e] (°C)
LDPE	0	200	7.7	119.5	n.d.
PE−HEMA 1	1.6	270	9.2	108.3	8.8
PE−HEMA 2	5.15	85	6.3	97.9	−0.3
PE−HEMA 3	6.8	37	3.8	91.5	−3.5
PE−HEMA 4	12.4	35	3.6	80.5	−10.8

[a]Determined via NMR. [b]Determined via GPC. [c]Decreasing molecular weight due to HEMA acting as chain transfer agent.[67] [d]Determined via DSC. [e]Determined via DMTA. For details, see the Methods section.

Table 2. Overview of Prepared ODIN−PE−HEMA Polymers

entry	parent polymer	ODIN[a] (mol %)	ODIN[b] (mol %)	T_m[d] (°C)	T_β[e] (°C)
P1	**PE−HEMA 1**	0.96	0.98	107.3	17.2
P2	**PE−HEMA 2**	2.16	2.25	95.5	20.0
P3	**PE−HEMA 3**	3.06[c]	3.45	86.5	33.0
P4	**PE−HEMA 4**	2.98[c]	6.05	79.4	48.2

[a]Determined via NMR. [b]Determined via EA. [c]Not fully dissolved in TCE-d_2 at 120 °C. [d]Determined via DSC. [e]Determined via DMTA.

signals of nonfunctional HEMA combine to a single peak after formation of the carbamate ($\delta \sim 4.3$ ppm). From the ratio of these two signals (nonfunctionalized and ODIN-functionalized HEMA) the degree of functionalization can be determined. About 40−60% of hydroxy groups underwent functionalization, with increasing reaction time having no considerable influence on grafting percentage.

For functional polymers **P3** and **P4**, ^{1}H NMR was not successful in determining the ODIN content due to only partial solubility in tetrachloroethane (TCE) at 120 °C. Therefore, elemental analysis (EA) was performed to determine the amount of incorporated ODIN. The EA determined ODIN content was in good agreement with the ^{1}H NMR determined content for soluble polymers **P1** and **P2** and will be used for subsequent comparison of these materials. Thereby, polymers with ODIN content ranging from 1 to 6 mol % could be obtained (Table 2). If we assume that the number of repeating units per chain does not change with functionalization, the average number of hydrogen bonding motifs per chains n_{HB} can be calculated according to the following relation:[70]

$$n_{HB} = \frac{M_n x_{HB}}{M_{HEMA} x_{HEMA} + M_{Et}(1 - x_{HEMA})} \quad (1)$$

with M_n as the number-average molecular weight of parent PE−HEMA, x_{HB} and x_{HEMA} as the molar fraction of ODIN (HB) and HEMA, and M_{HEMA} and M_{Et} as the molecular weight of HEMA and ethylene. According to eq 1, n_{HB} was determined to be 9.9, 9.5, 9.5, and 14.3 for polymers **P1**, **P2**, **P3**, and **P4**, respectively. Given that there are many more than two moieties per chain, a supramolecular network should be formed as long as the association of dimers is thermodynamically favored.

Hydrogen Bonding in ODIN−PE−HEMA Polymers. The influence of the introduction of the multiple hydrogen bonding moieties was investigated via DSC measurements on functional polymers (graphs in Figure S4). Compared to the pristine polymers, T_m and ΔH_m of functionalized materials decrease. The bulky motif grafted onto the polymer backbone hinders crystallization of the polymer main chain, reducing crystallinity and T_m.[38,71−73] In addition, T_β increases for each

DOI: 10.1021/acs.macromol.8b01715
Macromolecules XXXX, XXX, XXX−XXX

of the samples after functionalization (see Tables 1 and 2). This is due to the multiple hydrogen bonding facilitated formation of physical cross-links between chains, known to restrict chain movement and therefore increasing T_g.[70,74,75]

To showcase the adaptable nature of the hydrogen bonding functionalized system, stress relaxation was performed on **P2** at 140 °C in tensile mode. A strain of 0.5% was applied to **P2**, and the resulting stress, normalized for the initial stress, was monitored over time (Figure S5). A slow decline of the normalized stress to 20% of the initial value is observed within 1000 s, with full relaxation expected to be reached within 10000 s. Even though relaxation is slow, the stress of the physically cross-linked material can relax over time. In addition, it was possible to prepare defect-free samples suitable for mechanical analysis via compression molding at 150 °C (Figure S6), revealing indeed adaptability of our hydrogen bonding network. Compression molded samples of **P1**−**P4** and their respective PE−HEMA counterparts were analyzed via DMTA.

The data obtained for **P2** and the corresponding **PE−HEMA 2** are presented in Figure 5A (DMTA graphs for **P1**−**P4** in addition to their respective pristine PE−HEMA polymers are given in Figure S7). In polyethylene and related

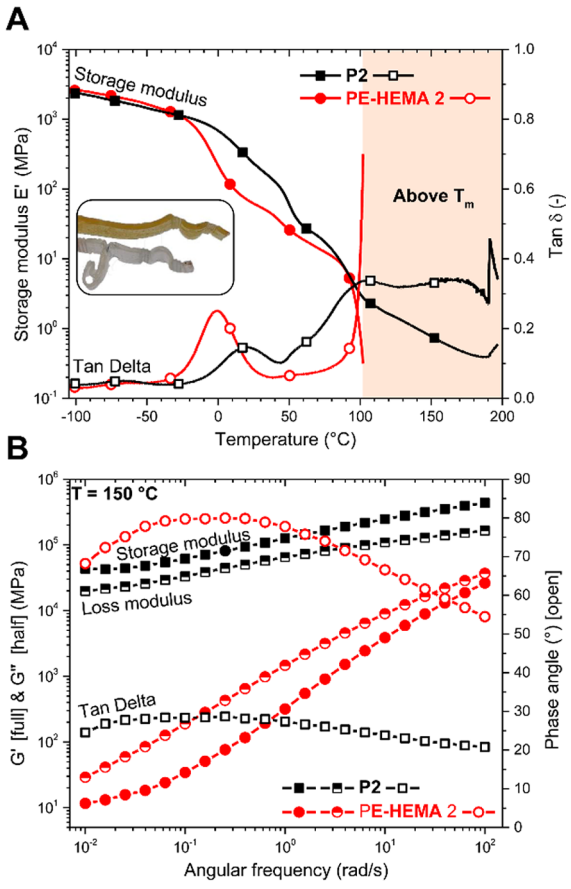

Figure 5. (A) DMTA sweep of **P2** (black) and **PE-HEMA 2** (red); E' is represented by closed symbols and δ by open symbols. The light red square highlights the temperature range above melting of the crystalline region; inset shows DMTA strips after measurements: **P2** (top) and **PE-HEMA 2** (bottom). (B) Rheology frequency sweep from 0.01 to 100 rad/s of **P2** (black) and **PE-HEMA 2** (red) at 150 °C. G' is represented by closed symbols, G'' by half symbols, and phase angle by open symbols.

copolymers such as the ones employed here, usually three main relaxations, α, β, and γ, are observed during DMTA. Specifically, α is close to the melting temperature, β close to room temperature, and γ below −100 °C, respectively.[76,77] The γ relaxation was not observed within the available measurement regime between −100 and 200 °C. A non-polyethylene related relaxation is observed for **P2**−**P4** and their corresponding pristine counterparts at −70 °C. Because no such transition is visible for **P1** and **PE−HEMA 1**, we believe that it is likely motion induced by breaking and re-forming hydrogen bonds of the HEMA side chain.[78] Associated with main chain movements in the amorphous region,[79] recent evidence denotes the β relaxation as the glass transition of polyethylene and its copolymers.[80] This relaxation has been found to change in intensity and location with the degree of crystallinity because of hindered amorphous chain segments as a result of the physical cross-links provided by the polymer crystallites.[81,82] Consequently, any types of additional branching points or cross-links should raise T_β. In fact, despite large molecular weight differences between pristine PE−HEMA polymers, DMTA determined ΔT_β increases linearly with ODIN content between pristine and functional polymers (Figure S8). This reflects a behavior previously observed for UPy functionalized methacrylate, where the glass transition increased linearly with UPy content for polymers of equal molecular weight.[83,84] A similar relationship is only partially verified for DSC determined ΔT_g because of the inaccuracy in evaluating T_g via DSC. The cross-links were still in effect for the region between T_β and T_α ($T > 50$ °C), where a greater E' was measured for **P2**−**P4**, with a less pronounced difference observed for **P1**.[85]

The α transition, usually related to main chain movements that become possible at the onset of melting of the crystalline phase,[76,82,86] is observed as a stark increase in tan δ for all of the pristine polymers until melting of the sample specimen leads to measurement stop. For functionalized samples, a more gradual increase of tan δ is observed leading into a peak for **P2**−**P4**, with tan δ of **P1** forming a shoulder around the melting temperature.

Remarkably, heating above T_m did not lead to measurement stop for functionalized samples, and the elastic character was retained, revealing a rubbery plateau after melting, characteristic for cross-linked polymers.[87−89] We attribute the formation of this plateau modulus to the cross-linking via multiple hydrogen bonding arrays, which is still effective above T_m. This was unexpected because these arrays of hydrogen bonds are expected to dissociate at elevated temperatures,[90] and adaptability of our network was apparent from stress relaxation measurements and from the possibility to obtain defect-free samples via compression molding. In contrast to cross-linked rubber, where E' usually remains constant above T_g,[91−93] E' decreases gradually after T_m up until 190 °C for functional polymers. At 190 °C, the polymer structure changes involving the formation of permanent cross-links, causing an increase in E', which will be discussed at a later stage. Because the hydrogen bonding moieties are in equilibrium between dissociated and associated states, we propose that the increasing temperature causes a shift from the dimeric to monomeric state, thus decreasing cross-link density.[52,75,84] The conformational stability of functional samples at elevated temperatures is easily visualized by looking at the DMTA sample strips after measurement displayed in the inset picture of Figure 5A. Melting compromised the shape of pristine

DOI: 10.1021/acs.macromol.8b01715
Macromolecules XXXX, XXX, XXX−XXX

(bottom), but not of functional sample (top). To investigate the properties of ODIN functional polymers in the melt state, **P2** was subjected to a frequency sweep at 150 °C, which is the temperature of compression molding, using parallel plate rheology, and compared to the pristine **PE-HEMA 2**. The data for both polymers are shown in Figure 5B. At 150 °C, the pristine sample (red line) was completely molten and displayed typical behavior of entangled polymer melts.[94] G'' is above G' over the entire frequency range, typical for non-cross-linked thermoplastics in the melt. No crossover point is observed for the pristine polymer within the measured frequency range, likely because it would occur outside of the measurement range. G'' and G' are strongly dependent on the observed time scale, displaying Newtonian-like flow behavior at long time scales (low frequencies) and more elastic behavior at short time scales (higher frequencies). However, the frequency sweep of the functional polymer reveals a completely different behavior. G' is above G'' over the entire frequency range, displaying solid, not melt-like, behavior. Additionally, the moduli are largely unaffected by frequency. Both are characteristic properties of cross-linked polymer systems, revealing the effective cross-linking via multiple hydrogen bonding in the melt.[94]

To confirm our theory that the multiple hydrogen bonding motifs are largely associated at elevated temperatures, variable temperature IR (VTIR) was performed. VTIR is a useful tool to investigate these types of interactions because the bands of amine and carbonyl groups involved in hydrogen bonding shift, as they dissociate.[35,95−97] VTIR was performed on **P3**, measuring first blank spectra as background and then taking spectra in intervals, starting from 25 °C up to 175 °C. These spectra are compared to ODIN functionalized reversible cross-linked Jeffamine T3000, a trifunctional polyether amine (JeffODIN; Figure S9). Here, functionalization of the liquid Jeffamine T3000 results in a supramolecular polymer able to form flexible films due to linkage of the low molecular weight species via sextuple hydrogen bonding. The VTIR spectra for JeffODIN and **P3** are shown in Figure 6. When looking at the temperature influence on the absorption peaks of JeffODIN, clear shifts are apparent in the C═O stretching and N−H bending region. Specifically, with increasing temperature the band at 1610 cm^{-1} loses intensity, and the absorption band observed at 1570 cm^{-1} shifts significantly toward lower wavenumbers. Together, these shifts indicate the progressive dissociation of hydrogen bonds at elevated temperature.[97] This is in line with visual observations, where viscous flow can be observed for JeffODIN starting at around 140 °C. On the contrary, for spectra of **P3**, only one peak can be observed to clearly change around 720 cm^{-1}, corresponding to the melting of PE crystalites.[98] No clear influence of temperature on peaks involved in hydrogen bonding is apparent for ODIN functionalized polymers. This can be attributed either to the influence of the apolar polymer matrix known to increase the strength of hydrogen bonds,[30,36] or by the cooperative associative effect due to the increased amount of moieties per chain. This effect was previously elucidated by Long et al., showing that more thermal energy was required to disrupt association of species with increasing numbers of UPy moieties.[99] Based on these results, multiple hydrogen bonding is clearly still in effect for ODIN functional polyolefin after melting of the crystalline regions and responsible for the observed plateau moduli after melting.

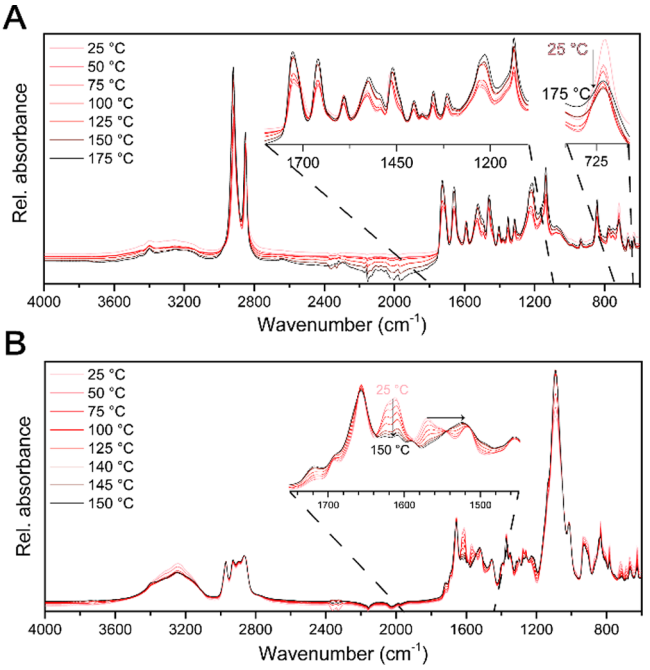

Figure 6. VTIR spectra of (A) ODIN functional polymer **P3** and (B) trifunctional supramolecular polymer JeffODIN. Samples were heated stepwise starting from 25 °C up to 150 °C in the case of JeffODIN and 175 °C for **P3**. The shifting absorption bands are indicated with arrows. Spectra are normalized for the C−H stretch region around 2830 cm^{-1}.

Thermal Stability of ODIN−PE−HEMA Polymers. One of the main motivations for developing the ODIN motif was the desired improved thermal stability over UPy functionalized polymers. To investigate the temperature of degradation, heat cycling DSC measurements were performed, repeatedly heating in steps of 10 °C/cycle from 160 to 250 °C using a heating rate of 10 K/min (Figure S10). The evolution of T_m was followed, and its shift was interpreted as degradation of the polymer structure. Indeed, for ODIN functionalized PE−HEMA, a T_m shift occurs at about 190 °C, placing the degradation temperature around 40 °C higher than the degradation temperature of UPy.[35,39] For some UPy functionalized polymer systems, thermal stability above 200 °C is claimed in the literature, based on TGA results alone.[51,100] Given the contradicting nature of these claims with other reported thermal stabilities of UPy functionalized polymers,[35] we suspected that TGA would give a false sense about the thermal stability of ODIN functional polymers, as it relates to the formation of volatiles.

To investigate whether TGA would report thermal stability higher than 190 °C for ODIN functionalized polymers, polymers **P3** and corresponding **PE-HEMA 3** were subjected to TGA and TGA-DSC measurements. Two major weight loss steps were observed for the functionalized polymer at 300 and 440 °C (Figure S11). During the first step, a mass loss of 24.76% was observed, in line with the theoretical weight loss of 24.58% for full abstraction of ODIN-motif in **P3**, cleaved at the carbamate linkage. Consequently, we surmise that during the first weight loss step ODIN and the linker chain degrade into volatiles, whereas the second weight loss step is caused by the polymer main chain degradation. This is coherent with the measurement of parent **PE-HEMA 3**, where only one weight loss step, in line with the second weight loss step of the

DOI: 10.1021/acs.macromol.8b01715
Macromolecules XXXX, XXX, XXX−XXX

functional polymer, was observed (Figure S12). No weight loss or peak in DSC-TGA was observed at 190 °C, the temperature of degradation determined via DSC.

As previously discussed, the urea group in UPy is thermoreversible, so that elevated temperature leads back to formation of amine and isocyanate species. Likewise, we assumed that the urea moiety of ODIN motif is thermoreversible. Therefore, thermal treatment of functional polymer species between 190 and 300 °C would not lead to degradation as such, but to formation of permanent cross-links facilitated by isocyanate−amine reactions. To investigate this theory, DMA was performed on **P4** at 190 °C, the degradation temperature determined via DSC, while monitoring E', E'', and tan δ as a function of time. **P4** was chosen because it has the largest amount of ODIN, and changes should be seen easily. The obtained data are shown in Figure 7. After 2 min at 190 °C, an increasing E' accompanied by a decrease of tan δ is observed. It is known that the formation of permanent cross-links is related to an increase in E'.[101] We can deduct that permanent cross-linking takes place in the polymer sample. We theorize that this is the result of re-formation of isocyanates and amines followed by immediate cross-linking of these species. On the basis of these results, together with results obtained from DSC and TGA, we believe that TGA alone cannot be the sole technique on which to claim thermal stability and structural integrity for these aryl urea type multiple hydrogen bonding species attached to polymers.

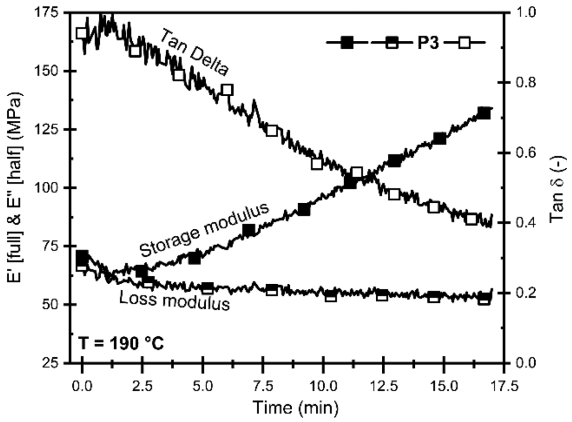

Figure 7. Graph of E', E'', and tan δ of **P3** measured in DMA tensile mode over 16 min at a constant temperature of 190 °C.

Tensile Properties of Functionalized Polymers. To assess the influence of cross-linking via ODIN on tensile properties, functionalized polymers **P1**−**P4** were subjected to tensile tests and compared to their respective pristine counterparts as well as the reference PE sample. The tensile strength and Young's modulus data for the measured polymers are given in Figure 8. Not shown are the data for strain at break, which generally decreases for functionalized polymers due to the formed cross-links.[102,103] The tensile strength of our reference LDPE material was within commonly obtained values.[104] For **P1**, no improved strength or increased stiffness was observed after functionalization, likely because of the reduced crystallinity of the functionalized sample without yet forming a strong enough hydrogen bonding network. For **PE-HEMA 2, 3, and 4**, however, the functionalization with ODIN tends to increase tensile strength and significantly increases stiffness of the soft polymers. The tensile strength of **PE-HEMA 4** was improved 3-fold, displaying the potential of ODIN motif to improve mechanical properties of polymeric species.[37] Interestingly, no improvement of tensile strength and only slightly increased stiffness were observed between **P3** and **P4**, despite the latter being functionalized with almost twice the amount of ODIN, revealing diminishing returns of ODIN functionalization. Compared to reference PE, tensile properties seem to be on par or slightly increased. This is due to the significantly reduced crystallinity of functionalized samples compared to the semicrystalline reference PE.[105]

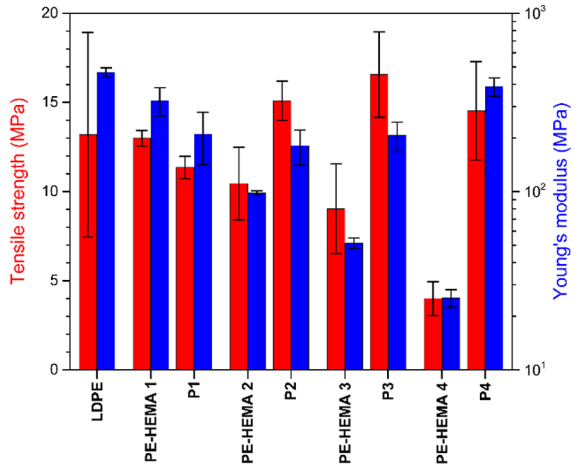

Figure 8. Measured average tensile strength and Young's modulus for reference LDPE, **P1**−**P4**, and related parent **PE**−**HEMA 1**−**4** polymers determined from at least three test specimens.

Multiple Hydrogen Bonding Cross-Linked Polyethylene as Oxygen Barrier Material. To reduce gas permeability through semicrystalline polymers, the free volume available for permeation may be reduced.[106] Reduction of the polymer free volume can be achieved by affecting either size or shape of polymer crystals or by reducing the chain mobility in the amorphous regions.[14] By introducing cross-links in the amorphous phase, the cohesive energy density between chains can be increased, which in turn reduces the oxygen permeability.[107] The formation of an efficient hydrogen bonding network should provide such cross-links resulting in increased barrier properties.

To investigate the effect of HEMA content and ODIN functionalization on the water and oxygen barrier properties, standard measurements[108] were performed to determine oxygen and water vapor transmission rates of selected polymers. The thickness corrected values for oxygen transmission obtained at 38 °C, 50% rh and water transmission measured at 23 °C, 85% rh are illustrated in Figure 9 (tabulated data and graph for oxygen transmission measured at 23 °C, 0% rh are reported in the Supporting Information). For PE−HEMA copolymers, a HEMA content dependent increase in both water and oxygen transmission rate is observed. This is due to the water penetrating the polymer matrix, revoking the interchain hydrogen bonds, therefore progressively affecting polymers with greater HEMA content.[14] By contrast, the measurements at near zero humidity reveal an almost constant oxygen transmission rate between different PE−HEMA polymers because the hydrogen bonding remains intact (Figure S13). The increased HEMA content should decrease the oxygen transmission due to network formation, but the advantageous effects are likely off set by the loss in crystallinity caused by the introduction of HEMA (see Figure S3). Upon

DOI: 10.1021/acs.macromol.8b01715
Macromolecules XXXX, XXX, XXX−XXX

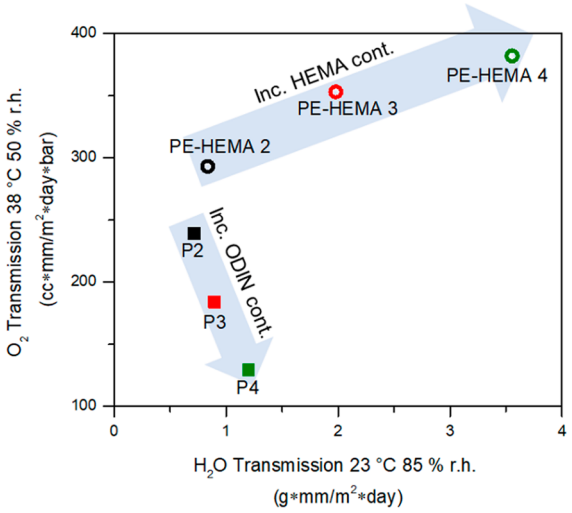

Figure 9. Oxygen and water vapor transmission rates of pristine and ODIN functional polymers. Oxygen transmission was measured at 38 °C, 50% rh and water vapor transmission at 23 °C, 85% rh. Corresponding pristine (open circles) and ODIN functional (closed squares) polymers share the same color. The arrows highlight the trend in transmission rates with respect to increasing HEMA and ODIN content for pristine and ODIN functional polymers.

functionalization of PE−HEMA polymers with ODIN, a gradual decrease in oxygen transmission is observed between pristine and functional polymers measured at 38 °C, 50% rh. Also, with increasing ODIN content, a lower oxygen transmission rate is detected, not being adversely affected by humidity in the same manner as pristine polymers with higher HEMA content were.

In addition, an almost equal water vapor transmission rate can be observed for all functional samples, showcasing the increased stability of these hydrogen bonding arrays toward humidity compared to single hydroxy hydrogen bonds.

CONCLUSIONS

Using the UPy motif, a plethora of multiple hydrogen bonding functionalized materials have been developed in the past 20 years. However, functionalization of polyolefins has been largely unexplored, with few examples including a fully amorphous LDPE material[37] and functional PP probed way above the degradation temperature of the UPy motif.[35,38] To overcome the thermal stability issues, the novel self-complementary multiple hydrogen bonding motif ODIN was developed. The structure of this new motif was elucidated via X-ray crystallography, revealing the formation of dimers in the solid state involving two regular and two bifurcated hydrogen bonds, resulting in a total of six hydrogen bonds. By reacting ODIN bearing pendant aliphatic isocyanate functionality with PE−HEMA, multiple hydrogen bonding array functionalized polyolefins with an ODIN content ranging from 1 to 6 mol % were obtained. The adaptable nature of the hydrogen bonding system was revealed via stress relaxation measurements and compression molding of thin films and sample strips. The formation of a cross-linked network was apparent from (i) the increased glass transition temperature determined via DMTA, (ii) the increased storage modulus of functionalized polymers above T_g, and (iii) the near frequency independent loss and storage moduli determined via parallel plate rheology. Remarkably, cross-linking via ODIN motif was still relevant after melting of the crystalline lattice, as revealed by parallel plate rheology and DMTA, where a rubbery plateau modulus was observed after melting, revealing a remarkably increased melt strength. This increased strength of hydrogen bonds is attributed to the apolar polymer matrix, elucidated via VTIR measurements. In comparison to UPy functionalized polymers, degradation involving permanent cross-linking of ODIN functional polyolefins occurs about 40 °C later. Moreover, compared to single hydrogen bonds, an increased resilience of the sextuple hydrogen bonding motif toward humidity was revealed during oxygen and water transmission measurements. For subsequent research, the influence of the polymer matrix must be considered in the design of multiple hydrogen bonding functionalized polymers. An appropriate matrix polymer could be used to tune the strength of hydrogen bonding moieties, making dimers with weaker association constants attractive choices. The increased thermal stability of ODIN should provide a useful tool for functionalization of polyolefins, but a key aspect will be to introduce moieties without adversely affecting the crystallinity of these polymers.

ASSOCIATED CONTENT

Supporting Information

The Supporting Information is available free of charge on the ACS Publications website at DOI: 10.1021/acs.macromol.8b01715.

Experimental data, synthesis of supramolecular polymer, NMR spectra, oxygen and water transmission data (PDF)

AUTHOR INFORMATION

Corresponding Authors

*(J.V.) E-mail: jerome.vachon@sabic.com.
*(E.D.) E-mail: enrico.dalcanale@unipr.it.

ORCID

Stefano Canossa: 0000-0002-6817-0810
Roberta Pinalli: 0000-0002-0000-8980
Enrico Dalcanale: 0000-0001-6964-788X

Notes

The authors declare no competing financial interest.

ACKNOWLEDGMENTS

This work is supported by the SUPRAmolecular polyolefins as oxygen BARRIER materials (SUPRABARRIER) Marie Skłodowska Curie project, which is funded through the European Union Eighth Framework Program (H2020-MSCA-ITN-2014) under the Grant Agreement No. 642929. We acknowledge Francesca Guagnini and Chiara Massera for their help in preparing suitable crystals. The financial support from SABIC is gratefully acknowledged. We thank Peter Neuteboom for providing the PE−HEMA polymers used in this study.

ABBREVIATIONS

PE−HEMA, poly(ethylene-*co*-(2-hydroxyethyl methacrylate)); PE, polyethylene; PP, polypropylene; DSC, differential scanning calorimetry; rh, relative humidity; UPy, ureidopyrimidinone; A, acceptor; D, donor; TGA, thermogravimetric analysis; DMTA, dynamic mechanical thermal analysis; ppm, parts per million; IR, infrared spectroscopy; VTIR, variable temperature infrared spectroscopy; EA, elemental analysis; TCE, tetrachloroethane; tan δ, tangent delta.

DOI: 10.1021/acs.macromol.8b01715
Macromolecules XXXX, XXX, XXX−XXX

REFERENCES

(1) Kauffman, G. B. History of Polyolefins: The World's Most Widely Used Polymers. *J. Chem. Educ.* **1986**, *63*, A181.
(2) Geyer, R.; Jambeck, J. R.; Law, K. L. Production, Use, and Fate of All Plastics Ever Made. *Sci. Adv.* **2017**, *3*, e1700782.
(3) Khanam, P. N.; AlMaadeed, M. A. A. Processing and Characterization of Polyethylene-Based Composites. *Adv. Manuf. Polym. Compos. Sci.* **2015**, *1*, 63−79.
(4) Pruitt, L. A. Deformation, Yielding, Fracture and Fatigue Behavior of Conventional and Highly Cross-Linked Ultra High Molecular Weight Polyethylene. *Biomaterials* **2005**, *26*, 905−915.
(5) Wannasri, S.; Panin, S. V.; Ivanova, L. R.; Kornienko, L. A.; Piriyayon, S. Increasing Wear Resistance of UHMWPE by Mechanical Activation and Chemical Modification Combined with Addition of Nanofibers. In *Procedia Engineering*; Elsevier: 2009; Vol. *1*, pp 67−70.
(6) Zhong, Y.; Janes, D.; Zheng, Y.; Hetzer, M.; De Kee, D. Mechanical and Oxygen Barrier Properties of Organoclay-Polyethylene Nanocomposite Films. *Polym. Eng. Sci.* **2007**, *47*, 1101−1107.
(7) Walker, A. M.; Tao, Y.; Torkelson, J. M. Polyethylene/Starch Blends with Enhanced Oxygen Barrier and Mechanical Properties: Effect of Granule Morphology Damage by Solid-State Shear Pulverization. *Polymer* **2007**, *48*, 1066−1074.
(8) Bhattacharyya, A.; Chen, S.; Zhu, M. Graphene Reinforced Ultra High Molecular Weight Polyethylene with Improved Tensile Strength and Creep Resistance Properties. *eXPRESS Polym. Lett.* **2014**, *8*, 74−84.
(9) Pietrasanta, Y.; Robin, J. J.; Torres, N.; Boutevin, B. Mechanical Performance Improvement of Low-Density Polyethylene Blends. *Mech. Time-Depend. Mater.* **1998**, *2*, 85−95.
(10) Xu, B.; Simonsen, J.; Rochefort, W. E. Mechanical Properties and Creep Resistance in Polystyrene/Polyethylene Blends. *J. Appl. Polym. Sci.* **2000**, *76*, 1100−1108.
(11) Garcia, D.; Starkweather, H. W. Hydrogen Bonding in Nylon 66 and Model Compounds. *J. Polym. Sci., Polym. Phys. Ed.* **1985**, *23*, 537−555.
(12) Fairley, G.; Prud'Homme, R. E. A Contribution to the Understanding of Polyethylene/Ionomer/Polyamide-6 Blends. *Polym. Eng. Sci.* **1987**, *27*, 1495−1503.
(13) Kollross, P.; Owen, A. J. The Influence of Hydrogen Bonding on Mechanical Anisotropy in Oriented Nylon-12. *Polymer* **1982**, *23*, 829−833.
(14) Mokwena, K. K.; Tang, J. Ethylene Vinyl Alcohol: A Review of Barrier Properties for Packaging Shelf Stable Foods. *Crit. Rev. Food Sci. Nutr.* **2012**, *52*, 640−650.
(15) Sheth, J. P.; Klinedinst, D. B.; Wilkes, G. L.; Yilgor, I.; Yilgor, E. Role of Chain Symmetry and Hydrogen Bonding in Segmented Copolymers with Monodisperse Hard Segments. *Polymer* **2005**, *46*, 7317−7322.
(16) Tsai, B. C.; Wachtel, J. A. Barrier Properties of Ethylene — Vinyl Alcohol Copolymer in Retorted Plastic Food Containers. In *Barrier Polymers and Structures*; American Chemical Society: Washington, DC, 1990; pp 192−202.
(17) Zhang, Z.; Britt, I. J.; Tung, M. A. Permeation of Oxygen and Water Vapor through EVOH Films as Influenced by Relative Humidity. *J. Appl. Polym. Sci.* **2001**, *82*, 1866−1872.
(18) Jia, N.; Fraenkel, H. A.; Kagan, V. A. Effects of Moisture Conditioning Methods on Mechanical Properties of Injection Molded Nylon 6. *J. Reinf. Plast. Compos.* **2004**, *23*, 729−737.
(19) Yang, B.; Huang, W. M.; Li, C.; Li, L. Effects of Moisture on the Thermomechanical Properties of a Polyurethane Shape Memory Polymer. *Polymer* **2006**, *47*, 1348−1356.
(20) Zimmerman, S. C.; Corbin, P. S. Heteroaromatic Modules for Self-Assembly Using Multiple Hydrogen Bonds. *Struct. Bonding (Berlin)* **2000**, *96*, 63−94.
(21) Park, T.; Zimmerman, S. C.; Nakashima, S. A Highly Stable Quadruply Hydrogen-Bonded Heterocomplex Useful for Supramolecular Polymer Blends. *J. Am. Chem. Soc.* **2005**, *127*, 6520−6521.
(22) Corbin, P. S.; Zimmerman, S. C.; Thiessen, P. A.; Hawryluk, N. A.; Murray, T. J. Complexation-Induced Unfolding of Heterocyclic Ureas. Simple Foldamers Equilibrate with Multiply Hydrogen-Bonded Sheetlike Structures. *J. Am. Chem. Soc.* **2001**, *123*, 10475−10488.
(23) Cheng, C.-C.; Huang, J.-J.; Liao, Z.-S.; Huang, S.-Y.; Lee, D.-J.; Xin, Z. Nucleobase-Functionalized Supramolecular Polymer Films with Tailorable Properties and Tunable Biodegradation Rates. *Polym. Chem.* **2017**, *8*, 1454−1459.
(24) Balkenende, D. W. R.; Monnier, C. A.; Fiore, G. L.; Weder, C. Optically Responsive Supramolecular Polymer Glasses. *Nat. Commun.* **2016**, *7*, 10995.
(25) Zhu, B.; Jasinski, N.; Benitez, A.; Noack, M.; Park, D.; Goldmann, A. S.; Barner-Kowollik, C.; Walther, A. Hierarchical Nacre Mimetics with Synergistic Mechanical Properties by Control of Molecular Interactions in Self-Healing Polymers. *Angew. Chem., Int. Ed.* **2015**, *54*, 8653−8657.
(26) Yamauchi, K.; Lizotte, J. R.; Long, T. E. Thermoreversible Poly(Alkyl Acrylates) Consisting of Self-Complementary Multiple Hydrogen Bonding. *Macromolecules* **2003**, *36*, 1083−1088.
(27) Faghihnejad, A.; Feldman, K. E.; Yu, J.; Tirrell, M. V.; Israelachvili, J. N.; Hawker, C. J.; Kramer, E. J.; Zeng, H. Adhesion and Surface Interactions of a Self-Healing Polymer with Multiple Hydrogen-Bonding Groups. *Adv. Funct. Mater.* **2014**, *24*, 2322−2333.
(28) Park, T.; Zimmerman, S. C. Formation of a Miscible Supramolecular Polymer Blend through Self-Assembly Mediated by a Quadruply Hydrogen-Bonded Heterocomplex. *J. Am. Chem. Soc.* **2006**, *128*, 11582−11590.
(29) Sijbesma, R. P.; Beijer, F. H.; Brunsveld, L.; Folmer, B. J.; Hirschberg, J. H.; Lange, R. F.; Lowe, J. K.; Meijer, E. W. Reversible Polymers Formed from Self-Complementary Monomers Using Quadruple Hydrogen Bonding. *Science* **1997**, *278*, 1601−1604.
(30) Folmer, B. J. B.; Sijbesma, R. P.; Versteegen, R. M.; Van Der Rijt, J. A. J.; Meijer, E. W. Supramolecular Polymer Materials: Chain Extension of Telechelic Polymers Using a Reactive Hydrogen-Bonding Synthon. *Adv. Mater.* **2000**, *12*, 874−878.
(31) Dankers, P. Y. W.; Hermans, T. M.; Baughman, T. W.; Kamikawa, Y.; Kieltyka, R. E.; Bastings, M. M. C.; Janssen, H. M.; Sommerdijk, N. A. J. M.; Larsen, A.; Van Luyn, M. J. A.; et al. Hierarchical Formation of Supramolecular Transient Networks in Water: A Modular Injectable Delivery System. *Adv. Mater.* **2012**, *24*, 2703−2709.
(32) Kieltyka, R. E.; Pape, A. C. H.; Albertazzi, L.; Nakano, Y.; Bastings, M. M. C.; Voets, I. K.; Dankers, P. Y. W.; Meijer, E. W. Mesoscale Modulation of Supramolecular Ureidopyrimidinone-Based Poly(Ethylene Glycol) Transient Networks in Water. *J. Am. Chem. Soc.* **2013**, *135*, 11159−11164.
(33) Söntjens, S. H. M.; Sijbesma, R. P.; Van Genderen, M. H. P.; Meijer, E. W. Stability and Lifetime of Quadruply Hydrogen Bonded 2-Ureido-4[1H]-Pyrimidinone Dimers. *J. Am. Chem. Soc.* **2000**, *122*, 7487−7493.
(34) Keizer, H. M.; van Kessel, R.; Sijbesma, R. P.; Meijer, E. W. Scale-up of the Synthesis of Ureidopyrimidinone Functionalized Telechelic Poly(Ethylenebutylene). *Polymer* **2003**, *44*, 5505−5511.
(35) Van Beek, D. J. M.; Spiering, A. J. H.; Peters, G. W. M.; Te Nijenhuis, K.; Sijbesma, R. P. Unidirectional Dimerization and Stacking of Ureidopyrimidinone End Groups in Polycaprolactone Supramolecular Polymers. *Macromolecules* **2007**, *40*, 8464−8475.
(36) Seiffert, S. *Supramolecular Polymer Networks and Gels*; Springer: 2015; Vol. *268*.
(37) Rieth, L. R.; Eaton, R. F.; Coates, G. W. Polymerization of Ureidopyrimidinone-Functionalized Olefins by Using Late-Transition Metal Ziegler-Natta Catalysts: Synthesis of Thermoplastic Elastomeric Polyolefins. *Angew. Chem.* **2001**, *113*, 2211−2214.
(38) Nojiri, S.; Yamada, H.; Kimata, S.; Ikeda, K.; Senda, T.; Bosman, A. W. Supramolecular Polypropylene with Self-Complementary Hydrogen Bonding System. *Polymer* **2016**, *87*, 308−315.
(39) Hoorne-van Gemert, G. M. L.; Janssen, H. M.; Meijier, E. W.; Bosman, A. W. Supramolecular Polymers from Low-Melting, Easily Processable Building Blocks, EP2087027A2, 2014, Suprapolix BV.

DOI: 10.1021/acs.macromol.8b01715
Macromolecules XXXX, XXX, XXX−XXX

(40) Nojiri, S.; Kimata, S.; Ikeda, K.; Senda, T.; Bosman, A. W.; Peeters, J. W.; Janssen, H. M. Novel Supramolecular Block Copolymer of Isotactic Polypropylene and Ethylene-Co-Propylene Connected by Complementary Quadruple Hydrogen Bonding System. *Macromolecules* **2017**, *50*, 5687−5694.
(41) Lausi, A.; Polentarutti, M.; Onesti, S.; Plaisier, J. R.; Busetto, E.; Bais, G.; Barba, L.; Cassetta, A.; Campi, G.; Lamba, D.; et al. Status of the Crystallography Beamlines at Elettra. *Eur. Phys. J. Plus* **2015**, *130*, 43.
(42) Contact Oxford Cryosystems; http://www.oxcryo.com/contact-us/ (accessed Feb 15, 2018).
(43) Rigaku Oxford Diffraction. CrysAlisPro Software System, Oxford, UK, 2017.
(44) Dolomanov, O. V.; Bourhis, L. J.; Gildea, R. J.; Howard, J. A. K.; Puschmann, H. IUCr. *OLEX2*: A Complete Structure Solution, Refinement and Analysis Program. *J. Appl. Crystallogr.* **2009**, *42*, 339−341.
(45) Anderson, C. A.; Taylor, P. G.; Zeller, M. A.; Zimmerman, S. C. Room Temperature, Copper-Catalyzed Amination of Bromonaphthyridines with Aqueous Ammonia. *J. Org. Chem.* **2010**, *75*, 4848−4851.
(46) Mayer, M. F.; Nakashima, S.; Zimmerman, S. C. Synthesis of a Soluble Ureido-Naphthyridine Oligomer That Self-Associates via Eight Contiguous Hydrogen Bonds. *Org. Lett.* **2005**, *7*, 3005−3008.
(47) Buhler, E.; Candau, S. J.; Schmidt, J.; Talmon, Y.; Kolomiets, E.; Lehn, J.-M. ibrillar Structure of Self-Assemblies Formed fromHeterocomplementary Monomers Linked throughSextuple Hydrogen-Bonding Arrays. *J. Polym. Sci., Part B: Polym. Phys.* **2007**, *45*, 103−115.
(48) Cheng, C.-C.; Yen, Y.-C.; Chang, F.-C. Hierarchical structures formed from self-complementary sextuple hydrogen-bonding arrays. *RSC Adv.* **2011**, *1*, 1190−1194.
(49) Beijer, F. H.; Sijbesma, R. P.; Kooijman, H.; Spek, A. L.; Meijer, E. W. Strong Dimerization of Ureidopyrimidones via Quadruple Hydrogen Bonding. *J. Am. Chem. Soc.* **1998**, *120*, 6761−6769.
(50) Armstrong, G.; Buggy, M. Thermal Stability of a Ureidopyrimidinone Model Compound. *Mater. Sci. Eng., C* **2001**, *18*, 45−49.
(51) Armstrong, G.; Buggy, M. Thermal Stability of Some Self-Assembling Hydrogen-Bonded Polymers and Related Model Complexes. *Polym. Int.* **2002**, *51*, 1219−1224.
(52) Lange, R. F. M.; Van Gurp, M.; Meijer, E. W. Hydrogen-Bonded Supramolecular Polymer Networks. *J. Polym. Sci., Part A: Polym. Chem.* **1999**, *37*, 3657−3670.
(53) Delebecq, E.; Pascault, J. P.; Boutevin, B.; Ganachaud, F. On the Versatility of Urethane/Urea Bonds: Reversibility, Blocked Isocyanate, and Non-Isocyanate Polyurethane. *Chem. Rev.* **2013**, *113*, 80−118.
(54) Ośmialowski, B.; Kolehmainen, E.; Kalenius, E.; Behera, B.; Kauppinen, R.; Sievänen, E. Intermolecular Steric Hindrance in 7-Acylamino-[1H]-2-Oxo-1,8- Naphthyridines: NMR, ESI-MS, IR, and DFT Calculation Studies. *Struct. Chem.* **2011**, *22*, 1143−1151.
(55) Jorgensen, W. L.; Pranata, J. Importance of Secondary Interactions in Triply Hydrogen Bonded Complexes: Guanine-Cytosine vs Uracil-2,6-Diaminopyndine. *J. Am. Chem. Soc.* **1990**, *112*, 2008−2010.
(56) Quinn, J. R.; Zimmerman, S. C.; Del Bene, J. E.; Shavitt, I. Does the A,T or G,C Base-Pair Possess Enhanced Stability? Quantifying the Effects of CH●●●O Interactions and Secondary Interactions on Base-Pair Stability Using a Phenomenological Analysis and ab Initio Calculations. *J. Am. Chem. Soc.* **2007**, *129*, 934−941.
(57) Skuches, G. S.; Carleton, P. S. Correlation of Urea Structure with Thermal Stability in Model Compounds. *J. Appl. Polym. Sci.* **1984**, *29*, 3431−3443.
(58) Wu, W.; Liu, Y.; Zhu, D. π-Conjugated Molecules with Fused Rings for Organic Field-Effect Transistors: Design, Synthesis and Applications. *Chem. Soc. Rev.* **2010**, *39*, 1489−1502.
(59) Allen, C. F. H. The Naphthyridines. *Chem. Rev.* **1950**, *47*, 275−305.
(60) Goswami, S.; Dey, S.; Gallagher, J. F.; Lough, A. J.; García-Granda, S.; Torre-Fernández, L.; Alkorta, I.; Elguero, J. Tailor-Made Naphthyridines: Self-Assembling Multiple Hydrogen-Bonded Supramolecular Architectures from Dimer to Helix. *J. Mol. Struct.* **2007**, *846*, 97−107.
(61) Stadler, R.; de Lucca Freitas, L. Thermoplastic Elastomers by Hydrogen Bonding 1. Rheological Properties of Modified Polybutadiene. *Colloid Polym. Sci.* **1986**, *264*, 773−778.
(62) de Lucca Freitas, L. L.; Stadler, R. Thermoplastic Elastomers by Hydrogen Bonding. 3. Interrelations between Molecular Parameters and Rheological Properties. *Macromolecules* **1987**, *20*, 2478−2485.
(63) Wolff, S. K.; Grimwood, D. J.; McKinnon, J. J.; Turner, M. J.; Javatilaka, D.; Spackman, M. A. *CrystalExplorer*; University of Western Australia: 2012.
(64) Biedermann, F.; Appel, E. A.; del Barrio, J.; Gruendling, T.; Barner-Kowollik, C.; Scherman, O. A. Postpolymerization Modification of Hydroxyl-Functionalized Polymers with Isocyanates. *Macromolecules* **2011**, *44*, 4828−4835.
(65) Farkas, A.; Strohm, P. F. Mechanism of Amine-Catalyzed Reaction of Isocyanates with Hydroxyl Compounds. *Ind. Eng. Chem. Fundam.* **1965**, *4*, 32−38.
(66) Patil, D. M.; Phalak, G. A.; Mhaske, S. T. Design and Synthesis of Bio-Based UV Curable PU Acrylate Resin from Itaconic Acid for Coating Applications. *Des. Monomers Polym.* **2017**, *20*, 269−282.
(67) Bhattacharyya, B. R.; Nandi, U. S. Determination of Chain Transfer of Alcohols by End Group Estimation. *Makromol. Chem.* **1968**, *116*, 8−13.
(68) Kautz, H.; Van Beek, D. J. M.; Sijbesma, R. P.; Meijer, E. W. Cooperative End-to-End and Lateral Hydrogen-Bonding Motifs in Supramolecular Thermoplastic Elastomers. *Macromolecules* **2006**, *39*, 4265−4267.
(69) Yan, X.; Li, S.; Pollock, J. B.; Cook, T. R.; Chen, J.; Zhang, Y.; Ji, X.; Yu, Y.; Huang, F.; Stang, P. J. Supramolecular Polymers with Tunable Topologies via Hierarchical Coordination-Driven Self-Assembly and Hydrogen Bonding Interfaces. *Proc. Natl. Acad. Sci. U. S. A.* **2013**, *110*, 15585−15590.
(70) Lewis, C. L.; Stewart, K.; Anthamatten, M. The Influence of Hydrogen Bonding Side-Groups on Viscoelastic Behavior of Linear and Network Polymers. *Macromolecules* **2014**, *47*, 729−740.
(71) Edward, G. H. Crystallinity of Linear Low Density Polyethylene and of Blends with High Density Polyethylene. *Br. Polym. J.* **1986**, *18*, 88−93.
(72) Cheng, J. J. Mechanical and Chemical Properties of High Density Polyethylene: Effects of Microstructure on Creep Characteristics, 2008.
(73) Hosoda, S.; Hori, H.; Yada, K.; Nakahara, S.; Tsuji, M. Degree of Comonomer Inclusion into Lamella Crystal for Propylene/Olefin Copolymers. *Polymer* **2002**, *43*, 7451−7460.
(74) Kuo, S. W.; Tsai, H. T. Complementary Multiple Hydrogen-Bonding Interactions Increase the Glass Transition Temperatures to PMMA Copolymer Mixtures. *Macromolecules* **2009**, *42*, 4701−4711.
(75) Jangizehi, A.; Ghaffarian, S. R.; Ahmadi, M. Dynamics of Entangled Supramolecular Polymer Networks in Presence of High-order Associations of Strong Hydrogen Bonding Groups. *Polym. Adv. Technol.* **2018**, *29*, 726−735.
(76) Kline, D. E.; Sauer, J. A.; Woodward, A. E. Effect of Branching on Dynamic Mechanical Properties of Polyethylene. *J. Polym. Sci.* **1956**, *22*, 455−462.
(77) Fan, W.; Wang, C.; Tsai, C.; Ding, Y.; Tu, Z.; Huang, C.-M.; Huang, K.-S.; Yeh, J. Ultradrawing Properties of Ultrahigh Molecular Weight Polyethylenes/Functionalized Activated Nanocarbon as-Prepared Fibers. *RSC Adv.* **2016**, *6*, 3165−3175.
(78) Pathmanathan, K.; Johari, G. P. Dielectric and Conductivity Relaxations in Poly(Hema) and of Water in Its Hydrogel. *J. Polym. Sci., Part B: Polym. Phys.* **1990**, *28*, 675−689.
(79) Sauer, J. A.; Woodward, A. E. Transitions in Polymers by Nuclear Magnetic Resonance and Dynamic Mechanical Methods. *Rev. Mod. Phys.* **1960**, *32*, 88−101.

DOI: 10.1021/acs.macromol.8b01715
Macromolecules XXXX, XXX, XXX−XXX

(80) Martín, S.; Vega, J. F.; Expósito, M. T.; Flores, A.; Martínez-Salazar, J. A Three-Phase Microstructural Model to Explain the Mechanical Relaxations of Branched Polyethylene: A DSC, WAXD and DMTA Combined Study. *Colloid Polym. Sci.* **2011**, *289*, 257−268.
(81) Nitta, K.; Tanaka, A. Dynamic Mechanical Properties of Metallocene Catalyzed Linear Polyethylenes. *Polymer* **2001**, *42*, 1219−1226.
(82) Schmieder, K.; Wolf, K. Mechanische Relaxationserscheinungen an Hochpolymeren - Beziehungen Zur Struktur. *Colloid Polym. Sci.* **1953**, *134*, 149−189.
(83) Lewis, C. L.; Stewart, K.; Anthamatten, M. The Influence of Hydrogen Bonding Side-Groups on Viscoelastic Behavior of Linear and Network Polymers. *Macromolecules* **2014**, *47*, 729−740.
(84) Feldman, K. E.; Kade, M. J.; Meijer, E. W.; Hawker, C. J.; Kramer, E. J. Model Transient Networks from Strongly Hydrogen-Bonded Polymers. *Macromolecules* **2009**, *42*, 9072−9081.
(85) Nielsen, L. E. Cross-Linking−Effect on Physical Properties of Polymers. *J. Macromol. Sci., Polym. Rev.* **1969**, *3*, 69−103.
(86) Oakes, W. G.; Robinson, D. W. Dynamic Electrical and Mechanical Properties of Polythene over a Wide Temperature Range. *J. Polym. Sci.* **1954**, *14*, 505−507.
(87) Zhou, Y.; Goossens, J. G. P.; Sijbesma, R. P.; Heuts, J. P. A. Poly(Butylene Terephthalate)/Glycerol-Based Vitrimers via Solid-State Polymerization. *Macromolecules* **2017**, *50*, 6742−6751.
(88) Röttger, M.; Domenech, T.; Van Der Weegen, R.; Breuillac, A.; Nicolaÿ, R.; Leibler, L. High-Performance Vitrimers from Commodity Thermoplastics through Dioxaborolane Metathesis. *Science* **2017**, *356*, 62−65.
(89) Mauri, M.; Tran, N.; Prieto, O.; Hjertberg, T.; Müller, C. Crosslinking of an Ethylene-Glycidyl Methacrylate Copolymer with Amine Click Chemistry. *Polymer* **2017**, *111*, 27−35.
(90) Wang, P. Ed.; *Smart Materials for Advanced Environmental Applications*; 2016.
(91) Jacob, M.; Francis, B.; Thomas, S.; Varughese, K. T. Dynamical Mechanical Analysis of Sisal/Oil Palm Hybrid Fiber-Reinforced Natural Rubber Composites. *Polym. Compos.* **2006**, *27*, 671−680.
(92) Shi, X. Y.; Bi, W. N.; Zhao, S. G. DMA Analysis of the Damping of Ethylene-Vinyl Acetate/Acrylonitrile Butadiene Rubber Blends. *J. Appl. Polym. Sci.* **2012**, *124*, 2234−2239.
(93) Geethamma, V. G.; Kalaprasad, G.; Groeninckx, G.; Thomas, S. Dynamic Mechanical Behavior of Short Coir Fiber Reinforced Natural Rubber Composites. *Composites, Part A* **2005**, *36*, 1499−1506.
(94) Goodyer, S. Measuring Polymers Using a Rotational Rheometer in Oscillatory Mode Product Manager for Rheology. *Telford Polym. Assoc.* **2013**, 1−35.
(95) Cheng, S.; Zhang, M.; Dixit, N.; Moore, R. B.; Long, T. E. Nucleobase Self-Assembly in Supramolecular Adhesives. *Macromolecules* **2012**, *45*, 805−812.
(96) Gellman, S. H.; Dado, G. P.; Liang, G. B.; Adams, B. R. Conformation-Directing Effects of a Single Intramolecular Amide-Amide Hydrogen Bond: Variable-Temperature NMR and IR Studies on a Homologous Diamide Series. *J. Am. Chem. Soc.* **1991**, *113*, 1164−1173.
(97) Zhang, K.; Aiba, M.; Fahs, G. B.; Hudson, A. G.; Chiang, W. D.; Moore, R. B.; Ueda, M.; Long, T. E. Nucleobase-Functionalized Acrylic ABA Triblock Copolymers and Supramolecular Blends. *Polym. Chem.* **2015**, *6*, 2434−2444.
(98) Hagemann, H.; Snyder, R. G.; Peacock, A. J.; Mandelkern, L. Quantitative Infrared Methods for the Measurement of Crystallinity and Its Temperature Dependence. Polyethylene. *Macromolecules* **1989**, *22*, 3600−3606.
(99) Elkins, C. L.; Viswanathan, K.; Long, T. E. Synthesis and Characterization of Star-Shaped Poly(Ethylene-Co-Propylene) Polymers Bearing Terminal Self-Complementary Multiple Hydrogen-Bonding Sites, 2006.
(100) Cao, K.; Liu, G. Low-Molecular-Weight, High-Mechanical-Strength, and Solution-Processable Telechelic Poly(Ether Imide) End-Capped with Ureidopyrimidinone. *Macromolecules* **2017**, *50*, 2016−2023.
(101) Charlesby, A.; Hancock, N. H. The Effect of Cross-Linking on the Elastic Modulus of Polyethylene. *Proc. R. Soc. London, Ser. A* **1953**, *218*, 245−255.
(102) Thompson, J. I.; Czernuszka, J. T. The Effect of Two Types of Cross-Linking on Some Mechanical Properties of Collagen. *Biomed. Mater. Eng.* **1995**, *5*, 37−48.
(103) Khonakdar, H. A.; Morshedian, J.; Wagenknecht, U.; Jafari, S. H. An Investigation of Chemical Crosslinking Effect on Properties of High-Density Polyethylene. *Polymer* **2003**, *44*, 4301−4309.
(104) Krishnaswamy, R.; Lamborn, M. Tensile Properties of Linear Low Density Polyethylene (LLDPE) Blown Films. *Polym. Eng. Sci.* **2000**, *40*, 2385−2396.
(105) Sarkhel, G.; Banerjee, A.; Bhattacharya, P. Rheological and Mechanical Properties of LDPE/HDPE Blends. *Polym.-Plast. Technol. Eng.* **2006**, *45*, 713−718.
(106) Ganesh, K.; Nagarajan, R.; Duda, J. L. Rate of Gas Transport in Glassy Polymers: A Free Volume Based Predictive Model. *Ind. Eng. Chem. Res.* **1992**, *31*, 746−755.
(107) Lagaron, J. M.; Catalá, R.; Gavara, R. Structural Characteristics Defining High Barrier Properties in Polymeric Materials. *Mater. Sci. Technol.* **2004**, *20*, 1−7.
(108) Barrier and Permeation Properties of Polymers and Plastics; http://www.intertek.com/polymers/barrier-properties/ (accessed Dec 22, 2017).

DOI: 10.1021/acs.macromol.8b01715
Macromolecules XXXX, XXX, XXX−XXX